Published in final edited form as:
Adv Healthc Mater. 2014 August ; 3(8): 1203–1209. doi:10.1002/adhm.201300611.

Carbon dots based two-photon visible nanocarriers for safe and highly efficient delivery of siRNA and DNA

Liqin Wang[#],
State Key Laboratory of Molecular Vaccinology and Molecular Diagnostics &Center for Molecular Imaging and Translational Medicine, School of Public Health, Xiamen University, Xiamen, 361102, China

Xiaoyong Wang[#],
State Key Laboratory of Molecular Vaccinology and Molecular Diagnostics &Center for Molecular Imaging and Translational Medicine, School of Public Health, Xiamen University, Xiamen, 361102, China

Ashwinkumar Bhirde,
Laboratory of Molecular Imaging and Nanomedicine, National Institute of Biomedical Imaging and Bioengineering, National Institutes of Health, Bethesda, MD 20892, USA

Jianbo Cao,
State Key Laboratory of Molecular Vaccinology and Molecular Diagnostics &Center for Molecular Imaging and Translational Medicine, School of Public Health, Xiamen University, Xiamen, 361102, China

Yun Zeng,
State Key Laboratory of Molecular Vaccinology and Molecular Diagnostics &Center for Molecular Imaging and Translational Medicine, School of Public Health, Xiamen University, Xiamen, 361102, China

Xinglu Huang,
Laboratory of Molecular Imaging and Nanomedicine, National Institute of Biomedical Imaging and Bioengineering, National Institutes of Health, Bethesda, MD 20892, USA

Yaping Sun,
Department of Chemistry and Laboratory for Emerging Materials and Technology, Clemson University, Clemson, South Carolina 29634, USA

Gang Liu[*], and
State Key Laboratory of Molecular Vaccinology and Molecular Diagnostics &Center for Molecular Imaging and Translational Medicine, School of Public Health, Xiamen University, Xiamen, 361102, China

Xiaoyuan Chen[*]
Laboratory of Molecular Imaging and Nanomedicine, National Institute of Biomedical Imaging and Bioengineering, National Institutes of Health, Bethesda, MD 20892, USA

[*]shawn.chen@nih.gov; gangliu.cmitm@xmu.edu.cn.

[#] These authors contributed equally to this work.

Abstract

The emergence of photoluminescent carbon-based nanomaterials offers great potential for a wide variety of biomedical applications such as fluorescence imaging and cellular labeling. This report illustrates a novel photonic carbon dot (Cdots) based nanocarrier by using low molecular weight amphiphilic PEI (Alkyl-PEI2k) for surface passivation. The resulting water-dispersible Alkyl-PEI2k-Cdot nanocarrier possesses good stability, monodispersity with narrow size distribution and fluorescence properties. In addition, Alkyl-PEI2k-Cdot nanocarrier has a markedly low toxicity and good gene transfection effect *in vitro* and *in vivo.* Considering its low cytotoxicity, high gene delivery efficiency and fluorescence performance, Alkyl-PEI2k-Cdots could serve as a novel imaging-trackable gene-delivery nanocarrier promising for gene therapy and optical molecular imaging.

Keywords

Carbon dots; gene delivery; polyethylenimine; RNA interference; plasmid DNA

1. Introduction

Gene therapy has shown a great potential in the treatment of genetic diseases, leading to the development of advanced medical methods. [1] However, gene therapeutic applications are limited mainly due to poor cellular uptake and accelerated degradation in biological fluids because naked DNA/siRNA gene is polyanionic in nature. [2] It is necessary to develop simple, safe and efficient strategies to transport the therapeutic gene into targeted cells for gene expression/silence. [3]

Conventionally viral vectors like adenovirus, retrovirus, herpes simplex virus and adeno-associated virus have been widely used to deliver therapeutic genes. [4] However, toxicity of the viral vectors has hindered the progress in this area. [5] To date, more and more researchers have turned their focus to the non-viral vectors. [6] Nanoparticle-based gene delivery systems offer an attractive alternative to viral vectors due to their biosafety, flexibility and ease of formulation and scale-up. [7] A number of organic/inorganic nanomaterials like iron oxide, manganese oxide, gold, hyaluronic acid nanoparticles have been used for gene loading/delivery and to overcome the extra- and intracellular barriers. [8, 9] Many of those nanomaterials have been well investigated for building up nanoparticle-based theranostics. [10] The functional nanomaterials not only can load and deliver gene effectively, but also can be tracked by different imaging techniques to develop new gene therapeutic protocols and guidelines. [10, 11]

Fluorescent nanoparticles have been widely investgated as gene delivery vectors since it is easy to track the delivery vehicle. [12] For example, quantum dots (Qdots) have been demonstrated as excellent siRNA delivery carriers. [13] However, Qdots have the issue of toxicity arising from the metal content and cannot be used *in vivo*. [14] Recently, carbon nanomaterials have been extensively studied as gene delivery vectors both *in vitro* and *in*

vivo. [15] Carbon nanotubes (CNTs) have been proven to be efficient gene delivery vectors because of their high cell penetrating ability. [16] Again toxicity of the CNTs has led to a road block towards translation aspect of CNT-based gene delivery system. [17] Recently fluorescent carbon nano-dots known as Cdots have emerged as an alternative to Qdots as non-metallic fluorescent probes. [18] Cdots have high photostability, tunable emission, and large two-photon excitation cross-sections exhibiting non-blinking fluorescence and excellent monodispersity, which show great potential in molecular imaging with minimal toxicity. [19, 20] However, without optimized surface modification, the gene may not bind strongly to Cdots, resulting in the instant release of the therapeutic gene during the delivery. For the application of Cdots in gene delivery, one choice of surface property is strongly positive charge to bind negatively charged DNA molecules *via* electrostatic interactions and release them after being internalized into tageted cells.

Cationic polymers have been widely employed as gene condensing agents to form positively charged, nanosized polyelectrolyte complexes, most popular among them is polyethylenimine (PEI). [21] PEI is a well-known transfection agent due to its superior buffering capacity, which allows excellent cargo translocation from endosomes to the cytoplasm by the “proton sponge” effect, and has been widely used to help penetrate the cancerous cells *in vitro*. [22] Recently, Liu *et al.* [23] developed a high-efficient gene vector based on PEI-passivated Cdots for *in vitro* gene transfection by using branched PEI25k. Generally, the molecular weight of PEI correlates strongly with its toxicity and transfection efficient. PEI25k is a highly effective gene transfection agent with high charge density that would limit the *in vivo* applications. The low molecular weight PEI, for example, PEI2k, shows excellent biocompatibility but low efficiency of gene delivery. However, low molecular weight PEI modified with hydrophobic parts (i.e., Alkyl-PEI2k) has been reported with high gene transfection efficiency and good biocompatibility. [9] We propose that Alkyl-PEI2k/Cdots nanocomposites (denoted as Alkyl-PEI2k-Cdots) may serve as a good photonic nanocarrier for *in vivo* gene delivery.

Therefore, in this study, we synthesized Alkyl-PEI2k-Cdots by using Alkyl-PEI2k for surface passivation and gene delivery (Figure 1). Our results showed that the nanovector possesses good stability, monodispersity with narrow size distribution and photoluminescence properties. We further found through agarose gel electrophoresis, toxicity and fluorescence performance studies, that Alkyl-PEI2k-Cdots is capable of stably binding, protecting, and delivering siRNA and plasmid DNA (pDNA) for potential gene therapy while maintaining fluorescence properties and high biocompatibility. Based on these systematic studies, we believe that Alkyl-PEI2k-Cdots with low cytotoxicity, high gene delivery efficiency and fluorescence properties, provide a safe and efficient avenue for gene therapy and optical molecular imaging.

2. Results and discussion

2.1 Characterization of Alkyl-PEI2k-Cdots

Inspired by progress with nanoparticle-based systems in gene delivery, in this study, we used a facile strategy to prepare Alkyl-PEI2k-Cdots which was slightly modified from our previously reported procedure. [24] After passivation with Alkyl-PEI2k, the zeta potential of

Cdots became 17.33 ± 1.97 mV, while the naked C-dots bearing negative charges had a zeta potential of around −20 mV, which confirmed the presence of amino group of the Alkyl-PEI2k on the surface of Cdots. As shown in Fig. 2A, scanning transmission electron microscopy (STEM) analysis of the Alkyl-PEI2k-Cdots sample found that the individual Cdots were well dispersed, with an average particle size of around 10 nm. The overall topographic analysis of the Cdots using atomic force microscope (AFM) showed the average height and length of the Cdots to be around 15 nm (Fig. 2B). The larger diameter of the Alkyl-PEI2k-Cdot determined by AFM may be caused by the AFM tip broadening effect and particle-flattening on the mica surface. To understand how the Alkyl-PEI2k-Cdots perform as optical imaging agents, we studied their fluorescence properties using an F-7000 fluorescence spectrophotometer. The fluorescence spectra of Alkyl-PEI2k-Cdots showed an emission peak at approximately 510 nm after excitation at 440 nm (Figure 2C). The imaging ability of Alkyl-PEI2k-Cdots in the visible and in the NIR range was also shown after excitation by a Maestro all-optical imaging system. Due to the unique physiochemical properties, Alkyl-PEI2k-Cdots show promise in accomplishing gene delivery with the necessary feature of visualizing the delivery.

2.2 Electrophoretic retardation analysis of Alkyl-PEI2k-Cdots

Positive charges are the most suitable surface charges for nanoparticles to be used in gene delivery [11]. The most attractive feature of the Alkyl-PEI2k modification for gene binding could be attributed to the electrostatic interactions between the amine groups of the polymer and phosphate groups of gene which eventually help form polyelectrolyte complexes. Thus, we propose that the positively charged surface of the Alkyl-PEI2k-Cdots has great potential to bind a large amount of negatively charged siRNA by utilizing electrostatic interactions. To evaluate the siRNA binding ability of Alkyl-PEI2k-Cdots, we mixed the particles with siRNA at varying nitrogen/phosphate (N/P) ratios and conducted the agarose gel electrophoresis and heparin decomplexation assay (Figure 3). As shown in Figure 3A, the migration of siRNA was completely retarded by the Alkyl-PEI2k-Cdots when N/P ratios are higher than 5. However, when heparin was added, siRNA was released from the complexes, indicating that siRNA can successfully bind to the surface of Alkyl-PEI2k-Cdots. Efficient complexation at low N/P ratio also suggests the strong binding ability of Alkyl-PEI2k-Cdots to siRNA. Meanwhile, as surrounded by the negatively charged siRNA, zeta potential of the Alkyl-PEI2k-Cdots complexes at different N/P ratios also decreased accordingly (Fig. 3C). The DLS results further confirmed that the siRNA was bound onto the surface of Alkyl-PEI2k-Cdots as the size distribution of nanocomplexes was increased to about 70 nm at N/P ratio of 2.5 (Fig. 3D).

2.3 Fluorescent imaging of Alkyl-PEI2k-Cdots in cancer cells

The fluorescent Cdots can be used for *in vitro* cell imaging with both one- and two-photon excitations, which has already been demonstrated in our previous reports. [19, 24] As shown in Fig. 4, Cdots were successfully taken up by the 4T1 cells after being mixed with Alkyl-PEI2k-Cdots/siRNA complexes as indicated by strong green fluorescence inside the cells. Both confocal laser scanning microscopy (CLSM) and two-photon fluorescence microscopy imaging found that Alkyl-PEI2k-Cdots were mainly in the cytoplasm. The results suggest that the carbon dots with strong fluorescence might offer great potential for imaging and

related biomedical applications, as deep imaging within tissue at micrometer resolution has become possible by the two-photon fluorescence microscopy. Transfected cells were washed, collected and embedded into gelatin phantom for fluorescence imaging by a Maestro all-optical imaging system. As shown in Fig. 4, cells transfected with Alkyl-PEI2k-Cdots/siRNA complexes resulted in stronger green fluorescence as compared to the controlled ones. Higher N/P ratios led to more polyplexes into cells, resulting in a higher amount of Cdots nanoparticle accumulation and stronger fluorescence effect.

2.4 *In vitro* transfection of Alkyl-PEI2k-Cdots/luciferase siRNA complexes

To further evaluate the potential of Alkyl-PEI2k-Cdots as siRNA carrier, firefly luciferase targeted siRNA were transfected with Alkyl-PEI2k-Cdots and gene expression was assessed by the measurement of enzyme activity. As shown in Fig. 5, the bioluminescence of 4T1-luc cells was inhibited significantly after treatment with Alkyl-PEI2k-Cdots/siRNA complexes, and the inhibition effect was similar to that of the commercially available Lipofectamine™ 2000. At the N/P ratio of 10, the transfection efficiency of Alkyl-PEI2k-Cdots/siRNA complexes was about twice of that at the N/P ratio of 2. This is probably due to the increase in the amine content in the nanoparticle/siRNA complexes. The higher amine content provides a higher buffering capacity to facilitate the endosomal escape of the siRNA into the cytoplasm. Interestingly, it was found that Alkyl-PEI2k-Cdots were able to transfect cells in both serum-free and -containing media, while Lipofectamine™ 2000 showed drastically reduced transfection ability if serum is added. It was expected that the formation of protein corona on the surface of Alkyl-PEI2k-Cdots, leading to the receptor-mediated endocytosis of Alkyl-PEI2k-Cdots/siRNA complexes. [11] All these data demonstrated that Alkyl-PEI2k-Cdots mediated effective delivery of siRNA into cells and resulted in remarkably efficient gene silencing.

Generally, the transfection efficiency and cytotoxicity of PEI correlate strongly with its molecular weight. [25] PEI-25k is a highly effective gene transfection agent with certain cytotoxicity, in comparison, lower molecular weight PEI such as PEI2k is more biocompatible. In the present study, the cytotoxicity of Alkyl-PEI2k-Cdots was assessed using a MTT cell viability assay after transfection treatment. Results shown in Fig. 6 indicate that the cytotoxicity of the Alkyl-PEI2k-Cdots/siRNA complexes is minimal compared to the other control groups even at the highest N/P ratio. The low cytotoxicity of Alkyl-PEI2k-Cdots/siRNA complexes could be ascribed to the low molecular weight as well as low density of amino groups in Alkyl-PEI2k. Thus, highly efficient down-regulation of luciferase was not due to the toxicity of the nanovector but rather the RNAi effect.

2.5 *In vitro* transfection of Alkyl-PEI2k-Cdots/luciferase DNA complexes

siRNA of 19-23 bp is difficult to be condensed and packed tightly by cationic agents because it is a topologically rigid molecule, while plasmid DNA (pDNA) molecules can be more easily condensed, packed and delivered by cationic agents. [26] *In vitro* transfection efficiency of Alkyl-PEI2k-Cdots/pDNA complexes was evaluated in 4T1 cells under serum-supplement conditions at N/P ratios from 2.5 to 10. The firefly luciferase gene was transfected with Alkyl-PEI2k-Cdots and gene expression was assessed by the measurement of enzyme activity. As shown in Fig. 7, when the 4T1 cells were treated with Alkyl-PEI2k-

Cdots/pDNA complexes, the bioluminescence of cells was significantly increased and the activation effect also showed an N/P ratio dependent behavior. The higher amine content could facilitate the endosomal escape of the pDNA into the cytoplasm, which can then be transported into the nucleus for luciferase gene expression. Furthermore, the low cytotoxicity of Alkyl-PEI2k-Cdots is perhaps beneficial to the *in vitro* pDNA transfection efficiency. All these data demonstrate that Alkyl-PEI2k-Cdots mediated effective gene delivery into cells result in remarkably efficient gene expression.

2.6 *In vivo* transfection of Alkyl-PEI2k-Cdots complexes and optical imaging

Since many nanovectors that transfect cells *in vitro* fail to function or have serious toxicity *in vivo*, Alkyl-PEI2k-Cdots nanocomplexes were directly injected into the tumor tissues to test whether Alkyl-PEI2k-Cdots could be used for *in vivo* gene delivery. The level of expression of luciferase reporter gene in fluc-4T1/4T1 xenograft tumors was tested by the IVIS imaging system 24 h after administration. Alkyl-PEI2k-Cdots/siRNA complexes (N/P ratio of 10, siRNA = 250 pmol/mouse) were directly injected into the fluc-4T1 tumor tissues. The gene-silencing effect was demonstrated as the relative level of luciferase expression was significantly reduced for the Alkyl-PEI2k-Cdots/siRNA complexes, but was not observed in the other control groups (Figure 8). Meanwhile, Alkyl-PEI2k-Cdots/ luciferase pDNA complexes (N/P ratio of 10, pDNA = 6 μg/mouse) were injected directly into the 4T1 tumor tissues. The significant bioluminescence of tumor demonstrates successful transfection by pDNA-loaded nanoparticles (Figure 9). In contrast, negligible signal was found in the control and free pDNA treatment of 4T1 tumor mice.

The intratumoral administration of Alkyl-PEI2k-Cdots/pDNA complexes showed no inhibition effects on tumor growth *in vivo*. In addition, no signs of granuloma formation were observed at intratumor administration sites. No change in the body mass or behavior of mice was observed up to 2 weeks following administration (data not shown). Taken together, our experimental results evidence the effective *in vitro* and *in vivo* gene transfection of Alkyl-PEI2k-Cdots.

Currently, molecular imaging has been pivotal in optimizing gene therapy and the ideal way to track the delivered genes in gene therapy is to use a specific imaging probe. To investigate the potential of Alkyl-PEI2k-Cdots as a promising tool for real-time gene tracking, *in vivo* fluorescence imaging was performed and our data showed that Alkyl-PEI2k-Cdots could serve as good fluorescent probes for *in vivo* gene tracking in live mice with good signal-to-background separation under NIR excitation (Figure 10). Due to the unique physiochemical properties, Alkyl-PEI2k-Cdots show promise in accomplishing gene delivery with the excellent feature of visualizing the delivery.

3. Conclusion

In summary, we successfully synthesized and characterized a new kind of gene delivery nanocarrier based on photonic Cdots by using Alkyl-PEI2k for surface passivation. Alkyl-PEI2k-Cdots possess good stability, monodispersity with narrow size distribution and photoluminescence properties. The cationic surface of the Alkyl-PEI2k-Cdots allows for effective gene binding *via* electrostatic interactions, leading to highly efficient gene delivery

in vitro and *in vivo* for potential gene therapy while maintaining the fluorescence properties and high biocompatibility of the Cdots. Our work highlights the promise of Alkyl-PEI2k-Cdots as a novel imaging-trackable nanocarrier for safe and efficient gene therapy and optical molecular imaging.

4. Experimental Section

4.1 Synthesis and surface passivation of Cdots

Functionalized Cdots were synthesized according to our previous reports [19, 24]. Briefly, the Cdots were synthesized *via* laser ablation of a carbon target in the presence of water vapor with argon. Then, Alkyl-PEI2k was used to react with the Cdots for surface passivation. Alkyl-PEI2k was mixed with an acid-treated particle sample, and the mixture was heated to 120 °C for 72 h. After the reaction, the mixture was cooled to room temperature and dispersed in water, followed by centrifugation for 30 min. The resulting particles were observed by transmission electron microscopy (TEM) and atomic force microscopy (AFM). The hydrodynamic size and zeta potential of the particles were measured using a SZ-100 Nano Particle analyzer (Horiba Scientific). The fluorescence spectra of nanoparticles were recorded on an F-7000 fluorescence spectrophotometer (Hitachi, Japan).

4.2 Agarose Gel Electrophoresis of Alkyl-PEI2k-Cdot/siRNA Complexes

Alkyl-PEI2k-Cdots/siRNA complexes were analyzed by 2% agarose gel electrophoresis and heparin decomplexation assay. The gels were prepared with 2% agarose in Tris-acetate-EDTA buffer containing 0.5 μg/mL ethidium bromide. Gel electrophoresis was carried out at 100 V for 15 min and the gel was subsequently imaged using a LAS-3000 gel documentation system (Fujifilm Life Science, Japan). For heparin decomplexation assay, Alkyl-PEI2k-Cdots were first complexed with siRNA (N/P ratio of 10) at room temperature for 20 min. Then, various amounts of heparin (heparin/siRNA weight ratio 0; 1; 5; 20 and 100) were added and the mixtures were further incubated for 15 min. The samples were loaded on a 2% agarose gel and subjected to electrophoresis as described above.

4.3 Cell Culture

The 4T1 murine mammary carcinoma cells were purchased from the American Type Culture Collection (ATCC). To establish 4T1 cell line that stably expresses luciferase gene (4T1-fluc), transfection was done with pcDNA 3.1 cytomegalovirus-firefly luciferase (fluc) DNA and Lipofectamine 2000 (Invitrogen) using 80% confluent 4T1 cells.[5] The cells were incubated for 48 h before the culture medium was changed. Selection was made by adding selective medium containing 1 mg/mL G418 antibiotic (Mediatech, Inc.) every 2-3 days. Two weeks later, the cells were analyzed and subcloned in 24-well plates. When reaching 80% confluence, the cells in the plate were imaged using a Xenogen IVIS-100 system (Caliper Life Sciences) after addition of the substrate D-luciferin (20 μL per well of 3 mg/mL stock). The 4T1-fluc clone with the highest fluc activity was selected for further studies. No significant difference between 4T1 and 4T1-fluc cells was observed in terms of proliferation or tumorigenicity. The cells were used when they reached 80% confluence.

4.4 Fluorescence microscopy imaging

Intracellular nanocomplexes were visualized by using fluorescence microscopes. 4T1 cells were seeded into the 35 mm culture dish with the glass bottom and transfected with Alkyl-PEI2k-Cdots/siRNA complex as mentioned above. Then, cells were fixed with 4% paraformalclehyde and observed with the Leica TCS SP5 confocal laser scanning microscopy (CLSM) imaging system (Leica, Germany). A Nikon fluoview multiphoton microscope (Nikon, Japan) was also used for two-photon luminescence imaging of the transfected cells using the multiphoton microscope with excitation at 810 nm. The laser power used for two-photon imaging was measured to be 1 mW at the focal plane. To quantify the relative fluorescence intensity of transfected cells, cells were washed, collected and embedded into gelatin phantom for fluorescence performance study by a Maestro all-optical imaging system.

4.5 *In vitro* transfection of Alkyl-PEI2k-Cdots/fluc siRNA complexes

fluc siRNA (6 pmol/well) and appropriate amount of Alkyl-PEI2k-Cdots were both diluted to 25 μL with fresh medium and were mixed at room temperature for 5 min; after that, the solution was incubated at room temperature for another 20 min. In the meantime, the fluc-4T1 cells in 96-well plate were washed with PBS and the medium was replaced with fresh medium (50 μL/well). The transfection complexes were then added into the wells and the cells were incubated at 37 °C, 5% CO_2, 95-100% humidity for the indicated time period. Cells for positive controls were transfected with Lipofectamine using the recommended protocol from the manufacturer (Invitrogen). The luciferase expression of fluc-4T1 cells was visualized 48 h post-transfection as described above. After transfection, the cytotoxicity of Alkyl-PEI2k-Cdots/siRNA complexes was evaluated using the standard MTT assay protocol. The relative percentage of the control (untreated) cells, which were not exposed to the transfection system, were used to represent 100% cell viability.

4.6 *In vitro* transfection of Alkyl-PEI2k-Cdots/fluc pDNA complexes

4T1 cells were seeded at a density of 3×10^4 cells/well in 12-well plate the day before use. Alkyl-PEI2k-Cdots/fluc pDNA complexes (N/P ratio of 2.5, 5, 7.5, 10; 2 μg pDNA/well) were incubated with the cells for 3 h in 100 μL of serum-free RPMI 1640 media followed by 48 h in 200 μL of RPMI 1640 media containing 10% FBS. The luciferase expression of 4T1 cells was visualized 48 h post-transfection as described above. Luminescent signal for each well was measured and plotted as average values.

4.7 *In vivo* studies

All *in vivo* animal procedures were approved by the Institutional Animal Care and Use Committee of Xiamen University. Xenografted tumor models were prepared by subcutaneous injection of 2×10^6 fluc-4T1/4T1 cells suspended in PBS into female athymic nude mice (6 weeks). When tumors reached about 6 mm in diameter, *in vivo* transfection of Alkyl-PEI2k-Cdots/siRNA or Alkyl-PEI2k-Cdots/fluc DNA complexes were tested by administering 250 pmol of siRNA or 6 μg of pDNA adsorbed to Alkyl-PEI2k-Cdots nanoparticles (N/P ratio of 10) intratumorally in 50 μL serum-free RPMI medium to anesthetized BALB/c mice, while the control group of mice received PBS, siRNA or pDNA

only. Before imaging, mice were anesthetized with a 2% isofluorane/air mixture and given a single intraperitoneally dose of 150 mg/kg D-luciferin in normal saline. Bioluminescence imaging was accomplished between 5 and 10 min post-luciferin administration. Signal intensity was quantified as the sum of all detected photon counts within a region of interest prescribed over the tumor site. The mice were imaged by a Maestro *in vivo* optical imaging system before and after intratumoral injection of Alkyl-PEI2k-Cdots nanocomplexes.

Acknowledgments

This work was supported by the Major State Basic Research Development Program of China (973 Program) (Grant Nos. 2013CB733802 and 2014CB744503), the National Natural Science Foundation of China (NSFC) (Grant Nos. 81101101, 81371596 and 51273165), the Key Project of Chinese Ministry of Education (Grant No. 212149), the Fundamental Research Funds for the Central Universities, China (Grant No. 2013121039), the Program for New Century Excellent Talents in University (NCET-13-0502), and the Intramural Research Program, National Institute of Biomedical Imaging and Bioengineering.

References

[1]. Fei Z, Wang S, Xie Y, Henslee BE, Koh CG, Lee LJ. Analytical chemistry. 2007; 79:5719. [PubMed: 17600386] Luo D, Saltzman WM. Nat Biotechnol. 2000; 18:33. [PubMed: 10625387] Mok H, Park TG. Biopolymers. 2008; 89:881. [PubMed: 18521895] Zhou X, Liu B, Yu X, Zha X, Zhang X, Wang X, Chen Y, Chen Y, Chen Y, Shan Y. Biomaterials. 2007; 28:4684. [PubMed: 17686512]

[2]. Gao X, Kim KS, Liu D. Aaps J. 2007; 9:E92. [PubMed: 17408239] Herweijer H, Wolff JA. Gene Ther. 2003; 10:453. [PubMed: 12621449] Medarova Z, Pham W, Farrar C, Petkova V, Moore A. Nat Med. 2007; 13:372. [PubMed: 17322898]

[3]. Segura T, Shea LD. Annu Rev Mater Res. 2001; 31:25.

[4]. Jang JH, Schaffer DV, Shea LD. Mol Ther. 2011; 19:1407. [PubMed: 21629221]

[5]. Schott JW, Galla M, Godinho T, Baum C, Schambach A. Curr Gene Ther. 2011; 11:382. [PubMed: 21787295]

[6]. Guo P. Nat Nanotechnol. 2010; 5:833. [PubMed: 21102465]

[7]. Srikanth M, Kessler JA. Nat Rev Neurol. 2012Li SD, Huang L. Gene Ther. 2006; 13:1313. [PubMed: 16953249]

[8]. Liu G, Choi KY, Bhirde A, Swierczewska M, Yin J, Lee SW, Park JH, Hong JI, Xie J, Niu G, Kiesewetter DO, Lee S, Chen X. Angew Chem Int Ed Engl. 2012; 51:445. [PubMed: 22110006] Xing R, Liu G, Quan Q, Bhirde A, Zhang G, Jin A, Bryant LH, Zhang A, Liang A, Eden HS, Hou Y, Chen X. Chem Commun (Camb). 2011; 47:12152. [PubMed: 21991584] Guo S, Huang Y, Jiang Q, Sun Y, Deng L, Liang Z, Du Q, Xing J, Zhao Y, Wang PC, Dong A, Liang XJ. ACS nano. 2010; 4:5505. [PubMed: 20707386] Yang R, Yang X, Zhang Z, Zhang Y, Wang S, Cai Z, Jia Y, Ma Y, Zheng C, Lu Y, Roden R, Chen Y. Gene Ther. 2006; 13:1714. [PubMed: 16838032]

[9]. Liu G, Xie J, Zhang F, Wang Z, Luo K, Zhu L, Quan Q, Niu G, Lee S, Ai H, Chen X. Small. 2011; 7:2742. [PubMed: 21861295]

[10]. Liu G, Swierczewska M, Lee S, Chen X. Nano Today. 2010; 5:524. [PubMed: 22473061]

[11]. Wang Z, Liu G, Zheng H, Chen X. Biotechnol Adv. 2013 doi: 10.1016/j.biotechadv.2013.08.020.

[12]. Jiang G, Park K, Kim J, Kim KS, Hahn SK. Mol Pharm. 2009; 6:727. [PubMed: 19178144]

[13]. Derfus AM, Chen AA, Min DH, Ruoslahti E, Bhatia SN. Bioconjug Chem. 2007; 18:1391. [PubMed: 17630789] Lee H, Kim IK, Park TG. Bioconjug Chem. 2010; 21:289. [PubMed: 20078095]

[14]. Soenen SJ, Demeester J, De Smedt SC, Braeckmans K. Biomaterials. 2012; 33:4882. [PubMed: 22494884] McConnachie LA, White CC, Botta D, Zadworny ME, Cox DP, Beyer RP, Hu X, Eaton DL, Gao X, Kavanagh TJ. Nanotoxicology. 2012Hoshino A, Hanada S, Yamamoto K. Arch Toxicol. 2011; 85:707. [PubMed: 21445587]

[15]. Kim H, Namgung R, Singha K, Oh IK, Kim WJ. Bioconjug Chem. 2011; 22:2558. [PubMed: 22034966] Liu M, Chen B, Xue Y, Huang J, Zhang L, Huang S, Li Q, Zhang Z. Bioconjug Chem. 2011; 22:2237. [PubMed: 21995530]

[16]. Al-Jamal KT, Gherardini L, Bardi G, Nunes A, Guo C, Bussy C, Herrero MA, Bianco A, Prato M, Kostarelos K, Pizzorusso T. Proc Natl Acad Sci U S A. 2011; 108:10952. [PubMed: 21690348]

[17]. Pacurari M, Qian Y, Fu W, Schwegler-Berry D, Ding M, Castranova V, Guo NL. J Toxicol Environ Health A. 2012; 75:129. [PubMed: 22251262]

[18]. Cao L, Yang ST, Wang X, Luo PG, Liu JH, Sahu S, Liu Y, Sun YP. Theranostics. 2012; 2:295. [PubMed: 22448196] Baker SN, Baker GA. Angew Chem Int Ed Engl. 2010; 49:6726. [PubMed: 20687055]

[19]. Sun YP, Zhou B, Lin Y, Wang W, Fernando KA, Pathak P, Meziani MJ, Harruff BA, Wang X, Wang H, Luo PG, Yang H, Kose ME, Chen B, Veca LM, Xie SY. J Am Chem Soc. 2006; 128:7756. [PubMed: 16771487]

[20]. Cao L, Wang X, Meziani MJ, Lu F, Wang H, Luo PG, Lin Y, Harruff BA, Veca LM, Murray D, Xie SY, Sun YP. J Am Chem Soc. 2007; 129:11318. [PubMed: 17722926] Yang ST, Cao L, Luo PG, Lu F, Wang X, Wang H, Meziani MJ, Liu Y, Qi G, Sun YP. J Am Chem Soc. 2009; 131:11308. [PubMed: 19722643] Yang ST, Wang X, Wang H, Lu F, Luo PG, Cao L, Meziani MJ, Liu JH, Liu Y, Chen M, Huang Y, Sun YP. J Phys Chem C Nanomater Interfaces. 2009; 113:18110. [PubMed: 20357893] Tao H, Yang K, Ma Z, Wan J, Zhang Y, Kang Z, Liu Z. Small. 2011; 8:281. [PubMed: 22095931]

[21]. Barua S, Ramos J, Potta T, Taylor D, Huang HC, Montanez G, Rege K. Comb Chem High Throughput Screen. 2011; 14:908. [PubMed: 21843141] Gunther M, Lipka J, Malek A, Gutsch D, Kreyling W, Aigner A. Eur J Pharm Biopharm. 2011; 77:438. [PubMed: 21093588] Dincer S, Turk M, Piskin E. Gene therapy. 2005; 12(Suppl 1):S139. [PubMed: 16231046]

[22]. Akinc A, Thomas M, Klibanov AM, Langer R. J Gene Med. 2005; 7:657. [PubMed: 15543529] Yezhelyev MV, Qi L, O'Regan RM, Nie S, Gao X. J Am Chem Soc. 2008; 130:9006. [PubMed: 18570415]

[23]. Liu C, Zhang P, Zhai X, Tian F, Li W, Yang J, Liu Y, Wang H, Wang W, Liu W. Biomaterials. 2012; 33:3604. [PubMed: 22341214]

[24]. Huang X, Zhang F, Zhu L, Choi KY, Guo N, Guo J, Tackett K, Anilkumar P, Liu G, Quan Q, Choi HS, Niu G, Sun YP, Lee S, Chen X. ACS Nano. 2013; 7:5684. [PubMed: 23731122]

[25]. Liu G, Wang Z, Lu J, Xia C, Gao F, Gong Q, Song B, Zhao X, Shuai X, Chen X, Ai H, Gu Z. Biomaterials. 2011; 32:528. [PubMed: 20869767]

[26]. Gary DJ, Puri N, Won YY. J Control Release. 2007; 121:64. [PubMed: 17588702]

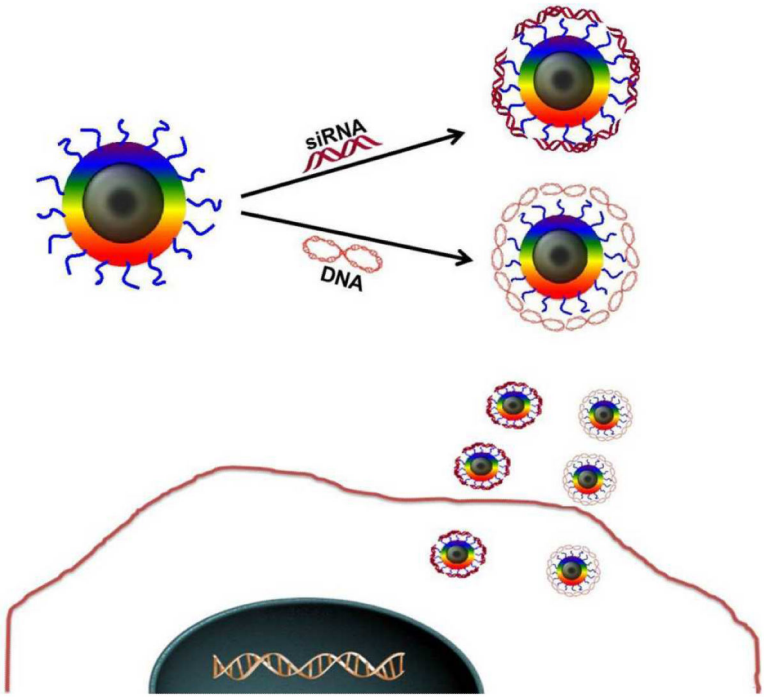

Figure 1.
Schematic showing the formation of Alkyl-PEI2k-Cdots/siRNA complex and delivery into cancer cell.

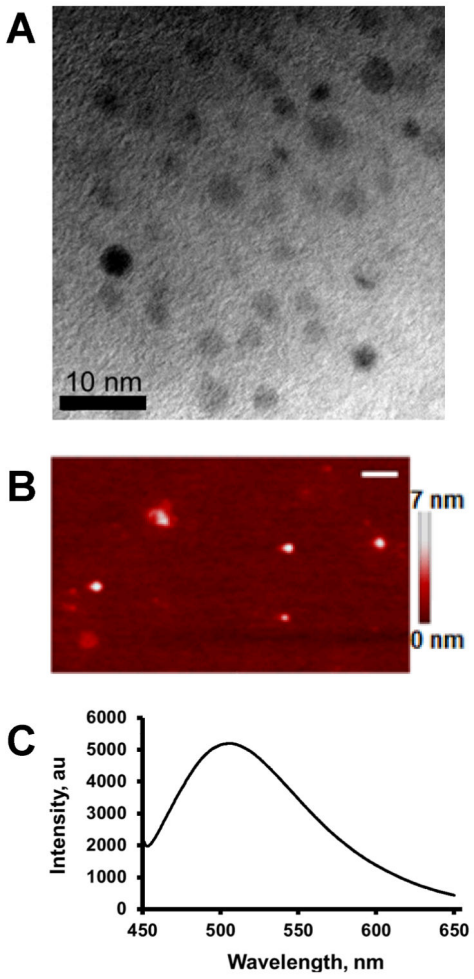

Figure 2.

(A) Scanning transmission electron microscopy and (B) atomic force microscopy image of Alkyl-PEI2k-Cdots (scale bar, 100 nm). (C) Fluorescence emission spectrum of Alkyl-PEI2k-Cdots.

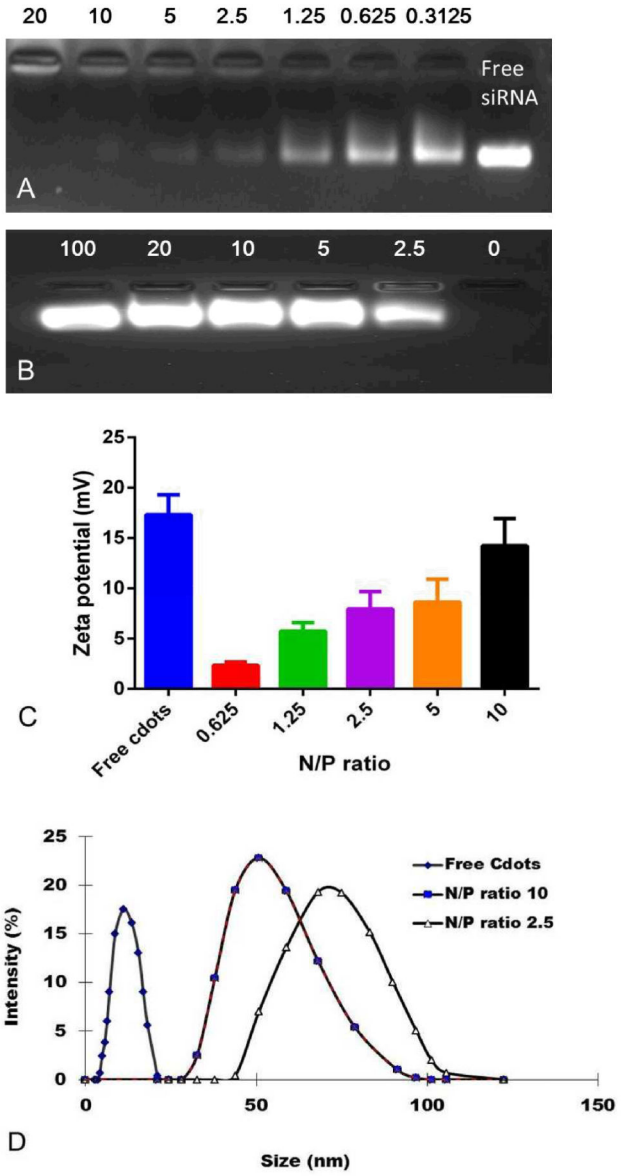

Figure 3.

Electrophoretic retardation analysis of Alkyl-PEI2k-Cdots. (A) siRNA binding assay: Alkyl-PEI2k-Cdots/siRNA complexes at different N/P ratios were prepared by adding an appropriate amount of Alkyl-PEI2k-Cdots into firefly luciferase siRNA (6 pmol) in PBS under agitation, and the mixture was incubated at room temperature for 20 min before Agarose gel electrophoresis. (B) siRNA release assay: Alkyl-PEI2k-Cdots were first complexed with siRNA (N/P ratio of 10) at room temperature for 20 min. Then, various amounts of heparin were added and the mixtures were further incubated for 15 min before Agarose gel electrophoresis. (C) Zeta potential and (D) size distribution of the Alkyl-PEI2k-Cdots/siRNA complexes at different N/P ratios.

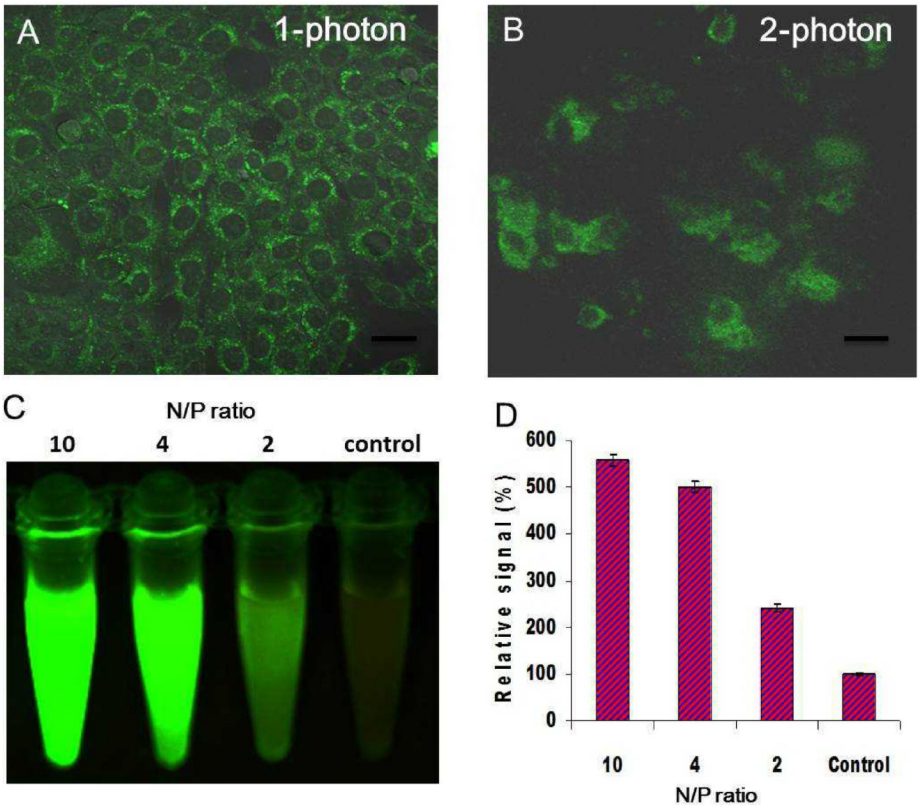

Figure 4.

(A) Confocal and (B) two-photon images of cells transfected with Alkyl-PEI2k-Cdots/siRNA complexes (N/P ratio of 10, scale bar 10 μm). (C) Higher N/P ratios correspond to images with stronger green fluorescence and thus more uptakes of the Cdots. (D) Quantification of fluorescence signal in (C).

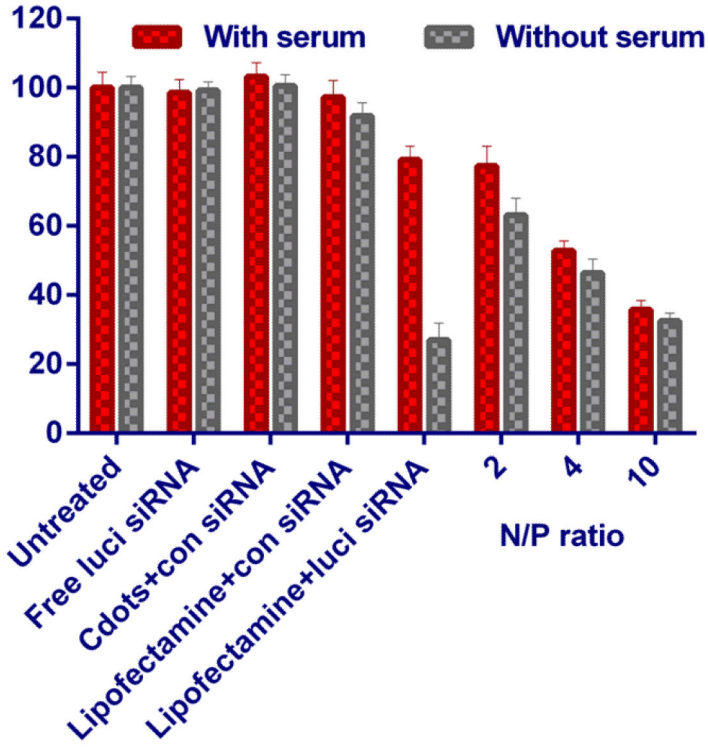

Figure 5.
Inhibition of fluc gene expression of fluc-4T1 cells by Alkyl-PEI2k-Cdots (siRNA = 6 pm) complexes at various N/P ratios.

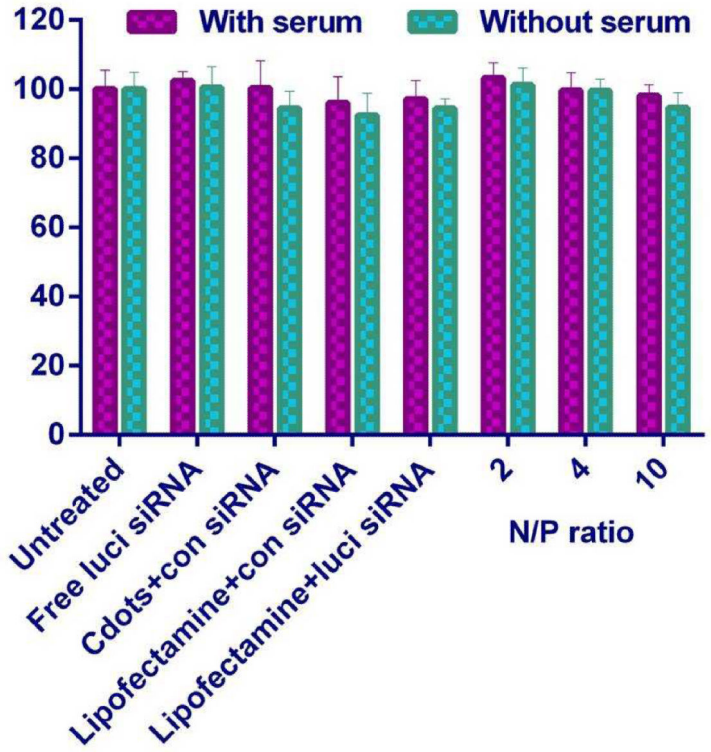

Figureure 6.
Cell viability assay of transfected 4T1 cancer cells treated with Alkyl-PEI2k-Cdots/siRNA complexes.

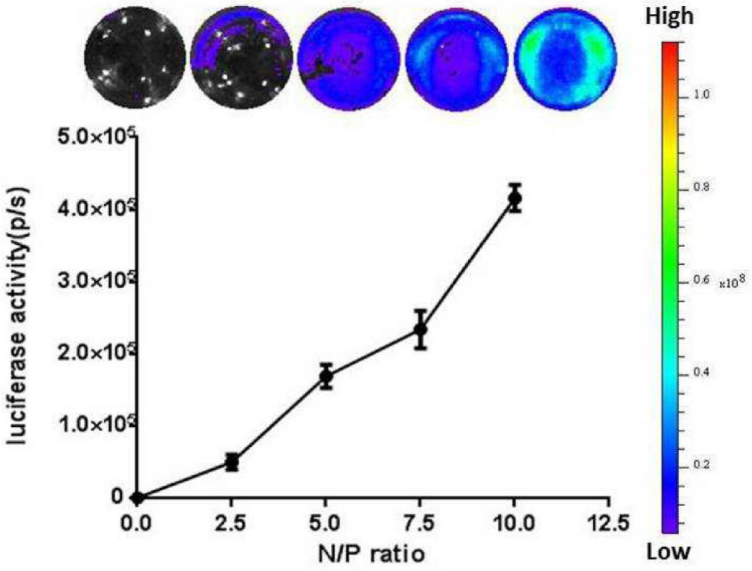

Figure 7.

In vitro pDNA gene transfection effect assessment with the firefly luciferase activity assay.

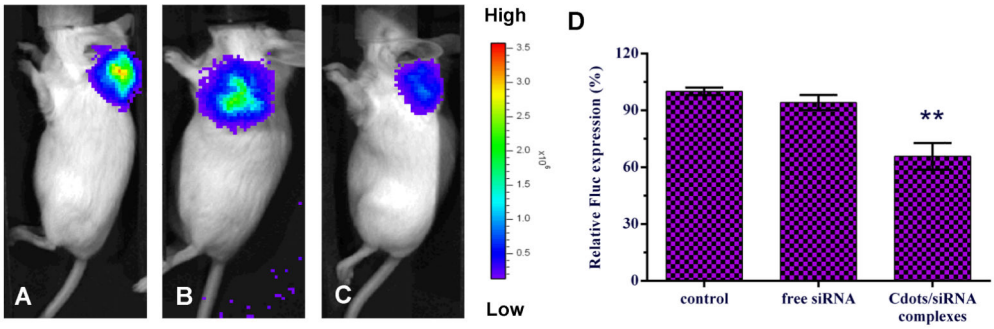

Figure 8.

In vivo optical images (A-C) and quantitative analysis (D) of luciferase gene expression after intratumoral injection of Alkyl-PEI2k-Cdots/siRNA complexes for fluc-4T1 xenograft. The decreased gene expression was confirmed with the administration of Alkyl-PEI2k-Cdots/siRNA complexes (C), while little to no gene-silence effect was found in the control (A) and free pDNA (B) treatment of these animals.

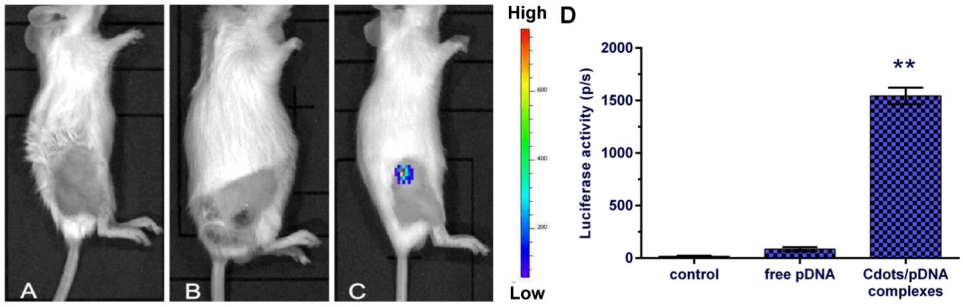

Figure 9.

In vivo optical images (A-C) and quantitative analysis (D) of luciferase gene expression after intratumoral injection of Alkyl-PEI2k-Cdots/pDNA complexes for 4T1 xenograft. The significant bioluminescence of tumor was confirmed with the administration of Alkyl-PEI2k-Cdots/pDNA complexes (C), while little to no signal above background was found in the control (A) and free pDNA (B) treatment of these animals.

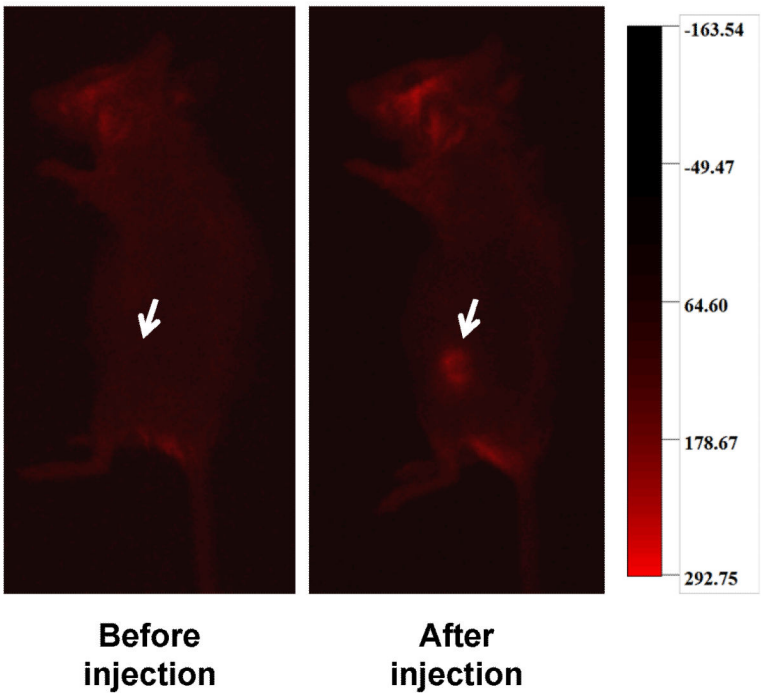

Figure 10.

In vivo fluorescence images of a mouse before and after intratumoral injection (arrows) of Alkyl-PEI2k-Cdots nanocomplexes.